IEEE Access
Multidisciplinary | Rapid Review | Open Access Journal

Received January 8, 2020, accepted January 26, 2020, date of publication February 6, 2020, date of current version February 26, 2020.

Digital Object Identifier 10.1109/ACCESS.2020.2972124

Clipping Noise Cancellation for Signal Detection of GSTFIM Systems

SHIWEN FAN[1,2], YUE XIAO[1], SHU FANG[1], YAN ZHAO[1], AND XIAOTIAN ZHOU[2]

[1]National Key Laboratory of Science and Technology on Communications, University of Electronic Science and Technology of China, Chengdu 611731, China
[2]Science and Technology on Communication Networks Laboratory, The 54th Research Institute of China Electronics Technology Group Corporation (CETC), Shijiazhuang 050000, China

Corresponding authors: Yue Xiao (xiaoyue@uestc.edu.cn) and Shu Fang (fangshu@uestc.edu.cn)

This work was supported in part by the National Science Foundation of China under Grant 61771106, in part by the Fundamental Research Funds for the Central Universities under Grant ZYGX2018J092, and in part by the Project from the Science and Technology on Communication Networks Laboratory, The 54th Research Institute of China Electronics Technology Group Corporation (CETC), under Grant JZX7Y201901SY001101.

ABSTRACT In this paper, a pair of clipping interference cancellation detectors based on symbol feedback and soft information are proposed for the generalized space-time-frequency index modulation (GSTFIM) systems. Specifically, the clipping interference is reconstructed by the prior information of the GSFTFIM symbol in these two detectors, then an iterative algorithm is developed for elimination and compensation of the clipping interference. The difference of these two proposed detectors lies in that the symbol feedback based interference cancellation (SFIC) detector completes the iteration through the hard decision symbol, while the soft information based interference cancellation (SIIC) detector iterates by the mean and variance of the estimated symbols. Simulation results show that the proposed two detectors can obtain flexible tradeoff between performance and complexity, compared to the traditional maximum likelihood (ML) detector with clipping interference.

INDEX TERMS Clipping, interference cancellation, generalized space-time-frequency index modulation (GSTFIM).

I. INTRODUCTION

Recently, a novel multiple-input multiple-output orthogonal frequency division multiplexing (MIMO-OFDM) system [1]–[4], termed as generalized space-time-frequency index modulation (GSTFIM) [5], was developed by conveying the information bits in the space-, time- and frequency-domains. In general, it originates from the concept of spatial modulation [6]–[8] and index modulation [9]–[11], while obtaining a balanced tradeoff between spectral efficiency and system performance compared to conventional MIMO-OFDM systems. Thus it can be considered as a powerful candidate for future wireless communications [12], [13].

Meanwhile, the high peak-to-average power ratio (PAPR) [14]–[16] of the transmitted symbols is a common issue of multi-carrier wireless communications including GSTFIM, due to the fact that it influences the power efficiency of hardware equipment and shortens the life of the terminal battery. In current researches, clipping [17], [18] is an effective way to solve the PAPR problem by limiting the power of the time-domain symbol below a preset threshold. In general, clipping has the advantages of simple operation, easy implementation and low complexity, and the disadvantages of additional interference in and out of the signal band [19], [20]. At the transmitting end, the out-of-band radiation problem can be solved by iterative filtering. However, at the receiving end, the in-band distortion caused by clipping must be handled in a certain way. For example, some interference cancellation algorithms [21]–[25] have been developed for OFDM systems. Furthermore, an iterative compensation detector for clipping noise was proposed in [26] for spatial modulation OFDM (SM-OFDM) systems. Moreover, the research on the clipping issue for the GSTFIM systems is still at an initial stage. Specifically, these detectors in [21]–[26] is conceived on the vector-by-vector based operation, which are not capable of employing to the GSTFIM systems due to the fact that the GSTFIM symbol is a matrix.

Against this background, we propose a pair of detectors based on the structure of GSTFIM symbol to solve the in-band distortion caused by clipping. Specifically, in the first proposed symbol feedback based interference cancellation (SFIC) detector, the estimated symbol in the time-domain is obtained by the hard decision based on the prior information. Then the estimated symbol in the frequency-domain and

The associate editor coordinating the review of this manuscript and approving it for publication was Usama Mir.

the decay component can be obtained by the the estimated symbol in the time-domain, which can be employed to get the estimation of additive clipping noise components. Finally, the posteriori information can be obtained by the additive clipping noise components and the received symbol. On the other hand, the process of the other proposed soft information based interference cancellation (SIIC) detector is described as follows. In the first step, the mean and variance of the GSTFIM symbols are calculated by the prior probability. In the second step, the damping matrix is obtained by the variance of the GSTFIM symbols. In the third step, the mean and variance of the clipping interference are calculated according to the calculated mean and variance of the GSTFIM symbols, and the damping matrix. In the fourth step, the posteriori information can be obtained by the mean and variance of the clipping interference. More details can be seen in the remainder of this paper. We show that the proposed SIIC detector can achieve better performance than SFIC due to the fact that it employs more information of the transmitted symbol, which is confirmed by simulation results.

The remainder of this paper is organized as follows. In section II, the clipping model for GSTFIM systems is introduced. Then in Section III, the proposed SFIC and SIIC detectors for clipping interference cancellation are introduced in detail, then the complexity analysis is presented. The simulation results are described in Section IV. Finally, in Section V, the conclusion is given.

Notation: The operators trace and $E(\cdot)$ represent the trace and expectation, respectively. $D(\cdot)$, $\angle$ and erfc $(\cdot)$ represent the variance, angle and complementary error function, respectively. $\binom{\mathrm{b}}{a}$ denotes the binomial coefficient. $||\cdot||_F$ denotes the Frobenius norm of a matrix. $abs(\cdot)$ denotes the absolute value function. $diag\left(\alpha_1, \alpha_2, \cdots, \alpha_{N_t}\right)$ denotes a diagonal matrix, whose diagonal elements is $\left(\alpha_1, \alpha_2, \cdots, \alpha_{N_t}\right)$.

II. CLIPPING MODEL FOR GSTFIM SYSTEM

According to [5], GSTFIM is a multi-carrier system with N subcarriers. All the N subcarriers are divided into K blocks, where each block has N_b subcarriers and only N_a out of N_b subcarriers are activated to realize the frequency index modulation, so the above processing can convey $b_1 = \left\lfloor \log_2 \binom{N_b}{N_a} \right\rfloor$ information bits, where $\lfloor\cdot\rfloor$ denotes the floor function. For the $k-th$ block subcarriers with $k = \{1, 2, \ldots K\}$, these symbols in the N_a activated subcarriers are called GSTSK symbols [27], while $N_b - N_a$ silent subcarriers formulate the zeros matrix. Specifically, the GSTSK symbol on the $i-th$ subcarrier with $i = 1, .., N_a$, equipped with N_t transmit antennas and T symbol durations, is generated by activating L out of Q dispersion matrices and selecting L M-PSK/QAM constellation symbols $s_1, s_2, \ldots, s_L$, expressed as

$$\mathbf{S}_i^k = \sum_{l=1}^{L} s_l \mathbf{A}_l^k \in \mathbb{C}^{N_t \times T}, \tag{1}$$

where $\mathbf{S}_i^k$ and $\mathbf{A}_l^k$ denote the GSTSK symbol on the $i-th$ subcarrier of the $k-th$ block and dispersion matrices, respectively. The above operations can modulate $\left\lfloor \log_2 \binom{Q}{L} \right\rfloor + L\log_2 M$ bits. Hence we use $b_2 = N_a\left(\left\lfloor \log_2 \binom{Q}{L} \right\rfloor + L\log_2 M\right)$ bits to modulate these N_a GSTSK symbols. In general, the GSTFIM symbol of the $k-th$ block can convey $b_k = b_1 + b_2$ information bits with $k = \{1, 2, \ldots K\}$. Thus, these GSTSK symbols $[\mathbf{S}_1^k, \mathbf{S}_2^k, \ldots, \mathbf{S}_{N_a}^k]^T$ on N_a subcarriers are mapped to $\mathbf{X}^k$ according to the information bits b_1 as follows,

$$\mathbf{X}^k = [\mathbf{X}_1^k,\ \mathbf{X}_2^k,\ \ldots,\ \mathbf{X}_{N_b}^k]^T. \tag{2}$$

Specifically, N_a elements of $\mathbf{X}^k$ are expressed as $[\mathbf{S}_1^k, \mathbf{S}_2^k, \ldots, \mathbf{S}_{N_a}^k]^T$, whose indices are written as $\mathbf{I}^k$, and other elements of $\mathbf{X}^k$ are zeros matrix.

Then, the frequency-domain transmitted symbols can be obtained by merging all the K block subcarriers as

$$\mathbf{X} = [\mathbf{X}^1, \mathbf{X}^2, \ldots, \mathbf{X}^K] \in \mathbb{C}^{NN_t \times T}. \tag{3}$$

Furthermore, the time-domain symbol $\mathbf{x} = [\mathbf{x}^1, \mathbf{x}^2, \ldots, \mathbf{x}^K] \in \mathbb{C}^{NN_t \times T}$ can be obtained by inverse fast Fourier transform (IFFT) as

$$\mathbf{x} = IFFT([\mathbf{X}^1, \mathbf{X}^2, \ldots, \mathbf{X}^K]). \tag{4}$$

For the $k-th$ block subcarriers, the clipping operation of $\mathbf{x}^k \in \mathbb{C}^{N_b N_t \times T}$ can be expressed as

$$\mathbf{s}_{(n,t)}^k = \begin{cases} Ae^{j\angle \mathbf{x}_{(n,t)}^k}, & \left|\mathbf{x}_{(n,t)}^k\right| > A \\ \mathbf{x}_{(n,t)}^k, & \left|\mathbf{x}_{(n,t)}^k\right| \leqslant A, \end{cases} \tag{5}$$

where $\mathbf{x}_{(n,t)}^k$ denotes the $(n,t)-th$ element of $\mathbf{x}^k$, $\angle \mathbf{x}_{(n,t)}^k$ denotes the angle of $\mathbf{x}_{(n,t)}^k$, $n = \{1, 2, \ldots, N_b T\}$ and $t = \{1, 2, \ldots, T\}$, A denotes the clipping threshold related to the clipping ratio γ, expressed as $A \triangleq \gamma\sqrt{c}$, where c denotes the sparsity of the GSTFIM symbol, $\mathbf{s}_{(n,t)}^k$ denotes the clipped symbol.

For the $k-th$ block subcarriers, the time-domain clipping symbol $\mathbf{s}^k \in \mathbb{C}^{N_b N_t \times T}$ can be obtained by traversing these indices as n and t of $\mathbf{s}_{(n,t)}^k$. Thus the clipped symbol $\mathbf{s} \in \mathbb{C}^{NN_t \times T}$ can be obtained by traversing all the blocks, expressed as

$$\mathbf{s} = [\mathbf{s}^1, \mathbf{s}^2, \ldots, \mathbf{s}^K] \in \mathbb{C}^{NN_t \times T}. \tag{6}$$

Then the cyclic prefix (CP) is added to $\mathbf{s}$. In the receiving end, after the operation of removing CP and fast Fourier transform (FFT), for the $l-th$ subcarrier, the frequency-domain clipping model can be expressed as

$$\mathbf{Y}_l = \mathbf{H}_l \bar{\mathbf{X}}_l + \mathbf{Z}_l, \tag{7}$$

where $l \in \{1, 2, \ldots, N\}$. The relation of the symbol between the $l-th$ of all the N subcarriers and the $n_b - th$ of the $k-th$ block subcarriers is $\bar{\mathbf{X}}_l = \bar{\mathbf{X}}_{n_b}^k$, where $k = \lfloor l/N_b \rfloor + 1$ and $n_b = \mathrm{mod}(l, N_b)$. And $\bar{\mathbf{X}}^k = [\bar{\mathbf{X}}_1^k, \bar{\mathbf{X}}_2^k, \ldots, \bar{\mathbf{X}}_{N_b}^k]^T$

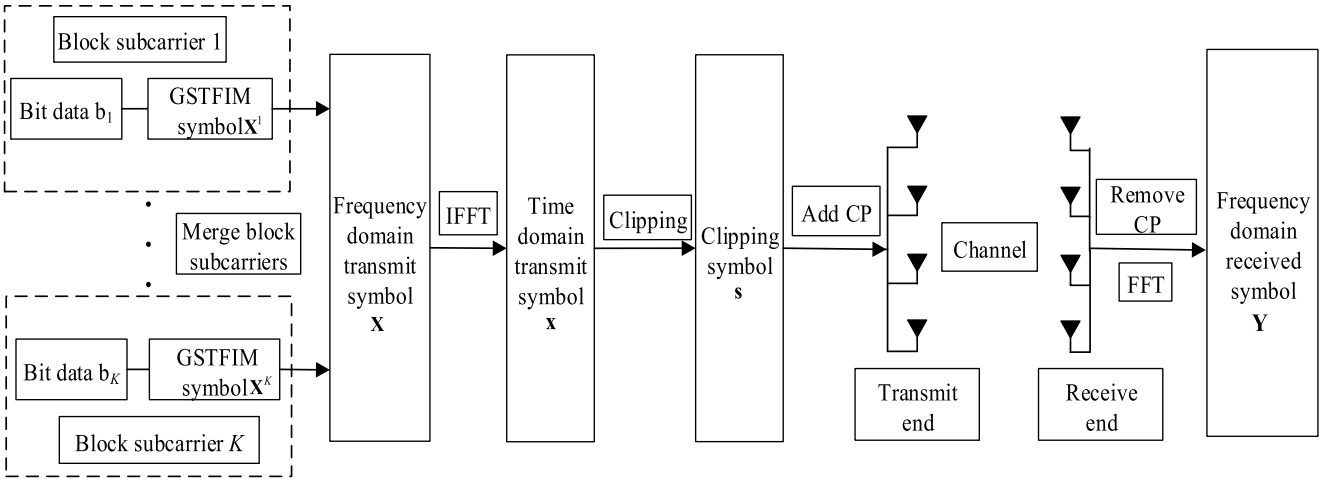

FIGURE 1. The clipping model for GSTFIM systems.

denotes the clipped frequency-domain symbol on the $k-th$ block subcarriers, which can be obtained by the FFT of the time-domain symbol $\mathbf{s}^k$.

According to [19], the clipped symbol $\mathbf{s}^k_{(n,t)}$ can be seen as the sum of the decay component of $\mathbf{x}^k_{(n,t)}$ and the additive clipping noise component based on the clipping operation (5), thus the frequency-domain symbol $\bar{\mathbf{X}}_l$ can be expressed as

$$\bar{\mathbf{X}}_l = \mathbf{B}_l \mathbf{X}_l + \mathbf{D}_l, \tag{8}$$

where $\mathbf{X}_l = \mathbf{X}^k_{n_b}$ denotes the frequency-domain symbol in (2), which satisfy $k = \lfloor l/N_b \rfloor + 1$ and $n_b = \mathrm{mod}(l, N_b)$. And $\mathbf{D}_l$ denotes the additive noise produced by clipping, $\mathbf{B}_l$ denotes the decay component, which is expressed as

$$\mathbf{B}_l = diag\left(\alpha_1, \alpha_2, \cdots, \alpha_{N_t}\right) \in \mathbb{R}^{N_t \times N_t}, \tag{9}$$

where

$$\alpha_t = 1 - e^{-\gamma^2} + \frac{\sqrt{\pi}\gamma}{2}\mathrm{erfc}\left(\gamma\right), \quad t \in (1, N_t). \tag{10}$$

Based on (6) and (7), the frequency-domain clipping model of GSTFIM systems can be reformulated as

$$\mathbf{Y}_l = \mathbf{H}_l \mathbf{B}_l \mathbf{X}_l + \mathbf{H}_l \mathbf{D}_l + \mathbf{Z}_l. \tag{11}$$

In general, the clipping model for GSTFIM systems is given in Fig. 1.

III. ITERATIVE CLIPPING INTERFERENCE CANCELLATION DETECTORS FOR GSTFIM SYSTEMS

In this subsection, to cancel the interference caused by clipping, two detectors termed as SFIC and SIIC are proposed. Specifically, our proposed detectors work in an iterative process. In the proposed SFIC detector, the bit data of $\mathbf{X}_l$ can be obtained by the prior information, which is employed to reconstruct the transmitted symbol $\hat{\mathbf{X}}_l$. Then the additive clipping noise component is estimated by $\hat{\mathbf{X}}_l$. Finally, the new received symbol is calculated by the received symbol minus the clipping noise component, which is employed to obtain the log likelihood rate (LLR) information based on the maximum posterior probability (MAP) detector. Thus the iteration of the information is completed. On the other hand, in the proposed SIIC detector, the mean and variance of $\mathbf{X}_l$ are obtained through the prior information, then they are employed to calculate the decay matrix, along with the mean and variance of the additive clipping noise. At last, the LLR information can be obtained by these above three parameters. More details are described as follows.

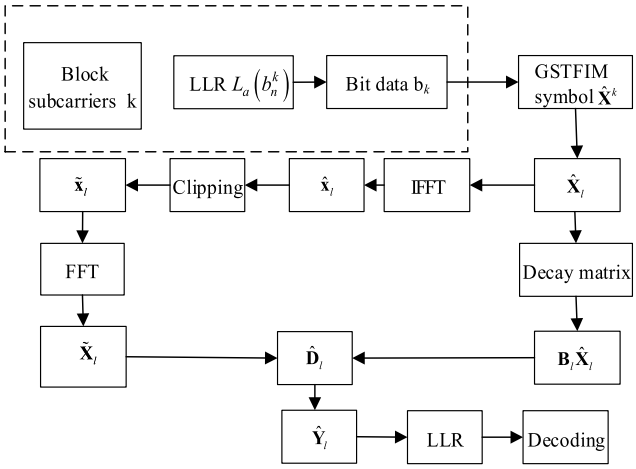

FIGURE 2. The flow chart of the SFIC detector for GSTFIM systems.

A. PROPOSED SFIC DETECTOR FOR GSTFIM SYSTEMS

The flow chart of the proposed SFIC detector can be seen in Fig. 1. The iterative process is as follows.

Step 1: At first, for the $k-th$ block, the bit data b_n^k is obtained by the LLR information $L_a\left(b_n^k\right)$, where $b_n^k \in \{0, 1\}$ and $n = \{1, 2, \ldots, b_k\}$.

Step 2: Compute the time-domain symbol $\hat{\mathbf{x}}_l$. The estimated symbol $\hat{\mathbf{X}}^k$ is calculated by the hard decision of the bit data b_n^k. Then the estimated symbol $\hat{\mathbf{X}}_l$ on the $l-th$ subcarrier is obtained through the mapping relation between the $n_b - th$

subcarrier of the $k-th$ block and the $l-th$ of all the N subcarriers, expressed as $l = n_b + N_b(k - 1)$. The time-domain symbol $\hat{\mathbf{x}}_l$ is calculated by the FFT of $\hat{\mathbf{X}}_l$.

Step 3: Estimate the additive clipping noise component $\hat{\mathbf{D}}_l$. The decay component $\mathbf{B}_l\hat{\mathbf{X}}_l$ is calculated by the estimated symbol $\hat{\mathbf{X}}_l$ and decay matrix $\mathbf{B}_l$ in (9). On the other hand, the time-domain symbol $\hat{\mathbf{x}}_l$ executes the clipping operation in (5) to obtain the clipping symbol $\tilde{\mathbf{x}}_l$. Then the frequency-domain symbol $\tilde{\mathbf{X}}_l$ can be obtained by the FFT of $\tilde{\mathbf{x}}_l$. Thus the clipping noise $\hat{\mathbf{D}}_l$ is expressed as

$$\hat{\mathbf{D}}_l = \tilde{\mathbf{X}}_l - \mathbf{B}_l\hat{\mathbf{X}}_l. \tag{12}$$

Step 4: The new received symbol can be expressed as

$$\hat{\mathbf{Y}}_l = \mathbf{Y}_l - \mathbf{H}_l\hat{\mathbf{D}}_l. \tag{13}$$

Step 5: Based on (11) and (13), the posteriori information of the $k-th$ block subcarriers can be calculated as

$$\Psi^k = \sum_{l=(k-1)N_b+1}^{kN_b} \frac{\left\|\hat{\mathbf{Y}}_l - \mathbf{H}_l\mathbf{B}_l\mathbf{X}_l\right\|_F^2}{\sigma^2}. \tag{14}$$

Step 6: According to the simplified criterion of the MAX-Log MAP algorithm, the LLR information is obtained as

$$L_e\left(b_n^k\right) = \max_{\mathbf{X}^k\in\mathbb{S}_1^n}\left[\Psi^k + \sum_{u\neq n}\left(b_u^k\right)L_a\left(b_u^k\right)\right] - \max_{\mathbf{X}^k\in\mathbb{S}_0^n}\left[\Psi^k + \sum_{u\neq n}\left(b_u^k\right)L_a\left(b_u^k\right)\right], \tag{15}$$

where $\mathbb{S}_0^n$ and $\mathbb{S}_1^n$ denote the valid subspace composed by the GSTFIM symbol, which satisfy $\mathbb{S}_0^n = \left\{\mathbf{X}^k \in \mathbb{S}^n : b_n^k = 0\right\}$ and $\mathbb{S}_1^n = \left\{\mathbf{X}^k \in \mathbb{S}^n : b_n^k = 1\right\}$, respectively.

Finally, the LLR information is de-interleaved and sent to the decoder. Thus we complete the Turbo equalization and decoding process.

B. PROPOSED SIIC DETECTOR FOR GSTFIM SYSTEMS

In the above SFIC detector, the feedback is achieved by hard decision, which will introduce some performance loss. In order to obtain more accurate cancellation of the clipping interference, the SIIC detector is proposed. Specifically, it employs the prior information to estimate the mean and variance of the transmitted symbols, and then they are employed to reconstruct the decay coefficient. On the other hand, the mean and variance of GSTFIM signals are used to estimate the mean and variance of the clipping noise component. Finally, the above two information is employed to obtain the LLR information and complete the iteration. The specific process is as follows.

Step 1: Compute the prior probability $P\left(\mathbf{X}^k = \alpha_i\right)$ of $\mathbf{X}_k$ based on the prior information $L_a\left(b_n^k\right)$. Assume that the corresponding bit information of GSTFIM symbol α_i is $\mathbf{c}_i = \{c_i^1, c_i^2, \ldots, c_i^{b_k}\}$, where $c_i^n \in \{0, 1\}$, $n = \{1, 2, \ldots, b_k\}$ and $i = \{1, 2, \ldots, 2^{b_k}\}$. Thus $P\left(\mathbf{X}^k = \alpha_i\right)$ is calculated as

$$P\left(\mathbf{X}^k = \alpha_i\right) = \prod_{n=1}^{b_k}\frac{e^{c_i^n L_a(b_n^k)}}{1 + e^{L_a(b_n^k)}}. \tag{16}$$

Step 2: Compute the mean of $\mathbf{X}_k$ as

$$E(\mathbf{X}^k) = \sum_{\alpha_i\in\mathbb{S}}\alpha_i P(\mathbf{X}^k = \alpha_i), \tag{17}$$

where $\mathbb{S}$ denotes the set of all the possible GSTFIM symbols, whose size is 2^{b_k}.

Compute the variance of $\mathbf{X}_k$ based on single carrier. Assume that $\mathbf{X}^k = [\mathbf{X}_1^k, \mathbf{X}_2^k, \ldots, \mathbf{X}_{N_b}^k]^T$, then the variance of $D(\mathbf{X}_{n_b}^k)$ is calculated as

$$D(\mathbf{X}_{n_b}^k) = \sum_{\alpha_i\in\mathbb{S}} P\left(\mathbf{X}^k = \alpha_i\right)\alpha_i^{n_b}(\alpha_i^{n_b})^H - E(\alpha_i^{n_b})E(\alpha_i^{n_b})^H, \tag{18}$$

where $\alpha_i^{n_b}$ denotes the symbol on the $n_b - th$ subcarrier of α_i, which is an $N_t \times T$ GSTSK symbol or zeros matrix. Thus the variance of $\mathbf{X}_k$ can be expressed as

$$D(\mathbf{X}^k) = [D(\mathbf{X}_1^k), D(\mathbf{X}_2^k), \ldots, D(\mathbf{X}_{N_b}^k)]^T. \tag{19}$$

Then the mean of all the above variance is expressed as

$$\bar{D} = \frac{1}{KN_b}\sum_{k=1}^{K}\sum_{n_b=1}^{N_b} D(\mathbf{X}_{n_b}^k). \tag{20}$$

Step 3: Compute the decay matrix $\mathbf{B}_k$. First, the new CR value γ_t is calculated as

$$\gamma_t = \frac{A}{\sqrt{\bar{D}(t,t)}} = \frac{\gamma\sqrt{c}}{\sqrt{\bar{D}(t,t)}}, \tag{21}$$

where $\bar{D}(t,t)$ denotes the $t-th$ diagonal element of the mean variance $\bar{D}$, where $t = \{1, 2, \ldots, N_t\}$. Thus the decay coefficient α_t is updated as

$$\alpha_t = 1 - e^{-{\gamma_t}^2} + \frac{\sqrt{\pi}\gamma_t}{2}\mathrm{erfc}\left(\gamma_t\right). \tag{22}$$

Traversing the index t of α_t from 1 to N_t, the decay matrix $\mathbf{B}_k$ can be obtained as

$$\mathbf{B}_k = diag\left(\alpha_1, \alpha_2, \cdots, \alpha_{N_t}\right). \tag{23}$$

Step 4: Compute the mean and variance of the clipping noise according to the mean and variance of $\mathbf{X}_k$. On one hand, the time-domain mean $E(\mathbf{x}^k)$ is obtained by the IFFT of $E(\mathbf{X}^k)$, then the time-domain clipped symbol $E(\tilde{\mathbf{x}}^k)$ is calculated by the clipping operation of $E(\mathbf{x}^k)$, finally the frequency-domain symbol $E(\tilde{\mathbf{X}}^k)$ can be obtained by the FFT of $E(\tilde{\mathbf{x}}^k)$.

On the other hand, assume that the mean $E(\mathbf{X}^k) = [E(\mathbf{X}_1^k), E(\mathbf{X}_2^k), \ldots, E(\mathbf{X}_{N_b}^k)]^T$, then the decay operation of $E(\mathbf{X}_{n_b}^k)$ can be expressed as

$$E(\bar{\mathbf{X}}_{n_b}^k) = \mathbf{B}_k E(\mathbf{X}_{n_b}^k), \tag{24}$$

where $n_b \in \{1, 2, \ldots, N_b\}$. The decay component of $E(\mathbf{X}^k)$ is obtained by traversing n_b from 1 to N_b as

$$E(\bar{\mathbf{X}}^k) = [E(\bar{\mathbf{X}}_1^k), E(\bar{\mathbf{X}}_2^k), \ldots, E(\bar{\mathbf{X}}_{N_b}^k)]^T. \tag{25}$$

Based on (8), (24) and (25), the mean of clipping noise $\hat{\mathbf{D}}^k$ is estimated as

$$E(\hat{\mathbf{D}}^k) = E(\bar{\mathbf{X}}^k) - E(\bar{\mathbf{X}}^k). \tag{26}$$

The variance $D(\hat{\mathbf{D}}^k)$ of the clipping noise is calculated as follows. Assume $E(\hat{\mathbf{D}}^k) = [E(\hat{\mathbf{D}}_1^k), E(\hat{\mathbf{D}}_2^k), \ldots, E(\hat{\mathbf{D}}_{N_b}^k)]^T$, thus the variance $\hat{\mathbf{D}}_{n_b}^k$ can be expressed as

$$D(\hat{\mathbf{D}}_{n_b}^k) = E\{\hat{\mathbf{D}}_{n_b}^k(\hat{\mathbf{D}}_{n_b}^k)^H\} - E(\hat{\mathbf{D}}_{n_b}^k)E(\hat{\mathbf{D}}_{n_b}^k)^H, \tag{27}$$

where $E\{\hat{\mathbf{D}}_{n_b}^k(\hat{\mathbf{D}}_{n_b}^k)^H\}$ is calculated as

$$E\{\hat{\mathbf{D}}_{n_b}^k(\hat{\mathbf{D}}_{n_b}^k)^H\} = \left(\mathbf{I}_{N_t} - \mathbf{G}\right) D(\mathbf{X}_{n_b}^k) - \mathbf{B}_k\mathbf{B}_k^H D(\mathbf{X}_{n_b}^k), \tag{28}$$

where $n_b = \{1, 2, \ldots, N_b\}$. $\mathbf{G}$ is denoted as

$$\mathbf{G} = diag(e^{-{\gamma_1}^2}, e^{-{\gamma_2}^2}, \cdots, e^{-{\gamma_{N_t}}^2}). \tag{29}$$

The variance $D(\hat{\mathbf{D}}^k)$ is obtained by traversing n_b as

$$D(\hat{\mathbf{D}}^k) = diag\{D(\hat{\mathbf{D}}_1^k), D(\hat{\mathbf{D}}_2^k), \ldots, D(\hat{\mathbf{D}}_{N_b}^k)\}. \tag{30}$$

Finally, the mean $E(\hat{\mathbf{D}}^k)$ and variance $D(\hat{\mathbf{D}}^k)$ of clipping noise in the $k-th$ block subcarriers are translated into $E(\hat{\mathbf{D}}^l)$ and variance $D(\hat{\mathbf{D}}^l)$ on the $l-th$ subcarrier according to the relationship $l = n_b + N_b(k\text{ - }1)$.

Step 5: For the $l-th$ subcarrier, the new received symbol can be expressed as

$$\hat{\mathbf{Y}}_l = \mathbf{Y}_l - \mathbf{H}_l E\left(\hat{\mathbf{D}}_l\right). \tag{31}$$

Based on (11) and (31), the posteriori information of the $k-th$ block subcarriers is calculated as

$$\Phi^k = \sum_{l=(k-1)N_b+1}^{kN_b} \frac{\left\|\hat{\mathbf{Y}}_l - \mathbf{H}_l\mathbf{B}_l\mathbf{X}_l\right\|_F^2}{\sigma_l^2}, \tag{32}$$

where σ_l^2 denotes the combined interference power of the additive white gaussian noise and the clipping noise, which is calculated as

$$\sigma_l^2 = \frac{\text{trace}\left[\text{abs}\left(D(\hat{\mathbf{D}}_l)\right)\right]}{N_t} + \sigma^2. \tag{33}$$

Step 6: Similar to (15), the LLR information is obtained as

$$L_e\left(b_n^k\right) = \max_{\mathbf{X}^k \in \mathbb{S}_1^n}\left[\Phi^k + \sum_{u\neq n}\left(b_u^k\right)L_a\left(b_u^k\right)\right] - \max_{\mathbf{X}^k \in \mathbb{S}_0^n}\left[\Phi^k + \sum_{u\neq n}\left(b_u^k\right)L_a\left(b_u^k\right)\right]. \tag{34}$$

The above LLR information is employed to the decoder, thus we has finished each iteration.

In general, we have proposed two detectors as SFIC and SIIC to reconstruct the GSTFIM symbol. The difference is that SFIC is realized by the hard decision of the GSTFIM symbol, while SIIC utilizes the mean and variance of the GSTFIM symbol. The SFIC has lower complexity, but its performance is descend due to the deletion of information. The SIIC has considered more information, thus it has better performance.

It is worth noting that the proposed SFIC and SIIC detectors are different from the detectors of [26] and [32]–[35] in the following two aspects: (a) The detectors of [26] and [32]–[35] are conceived for SM-OFDM and MIMO systems, respectively, which are calculated on the vector-by-vector based operation. While, the propose detectors are conceived for GSTFIM systems, which are derived on the spatial- and time-domain based matrix operation. Specifically, the proposed detectors are derived based on the matrix $\mathbf{X}_l \in \mathbb{C}^{N_t\times T}$ rather than on the vector $\mathbf{x}_k \in \mathbb{C}^{N_t\times 1}$. In other word, the basic unit is the spatial- and time-domain symbol in the proposed detectors instead of the spatial-domain symbol in [26] and [32]–[35]. Furthermore, the GSTFIM symbol $\mathbf{X}^k \in \mathbb{C}^{N_tN_b\times T}$ contains zeros matrix, which is not included in the MIMO system; (b) The posteriori information of the proposed SFIC and SIIC detectors is obtained by combining

$$C_{SFIC} = \underbrace{4N_tTN}_{(12)} + \underbrace{8N_rN_tTN}_{(13)} + \underbrace{(2N_rN_t + 8N_rN_tT + 4N_rT)(2^{b_3}+1)N + (N_b-1)K}_{(14)} + \underbrace{(4b_k-3)Kb_k}_{(15)} \tag{35}$$

$$\begin{aligned} C_{SIIC} = {} & \underbrace{(6b_k-1)2^{b_k}}_{(16)} + \underbrace{2N_tN_bT(2^{b_k+1}-1)}_{(17)} + \underbrace{(8TN_t^2 2^{b_3} + 2N_t^2 2^{b_k} - 2N_t^2 + 8TN_t^2)N}_{(18)} + \underbrace{2N_t^2KN_b}_{(20)} \\ & + \underbrace{4N_t}_{(21)} + \underbrace{9N_t}_{(22)} + \underbrace{2N_tTN}_{(24)} + \underbrace{2KN_bN_tT}_{(26)} + \underbrace{8TN_t^2N}_{(27)} + \underbrace{(6N_t^2+2N_t)N}_{(28)} + \underbrace{8N_rN_tTN}_{(31)} \\ & + \underbrace{(2N_rN_t + 8N_rN_tT + 4N_rT)(2^{b_3}+1)N + (4b_k-3)Kb_k}_{(32)} \\ & + \underbrace{(N_t+1)N}_{(33)} + \underbrace{(4b_k-3)Kb_k}_{(34)} \end{aligned} \tag{36}$$

N_b subcarriers probabilities of (14) and (32) on the $k-th$ block subcarriers, respectively, while in [32] and [34], it is obtained by the probability of single transmit antenna. And in [26], [33] and [35], the posteriori information is obtained by the probability of single subcarrier.

IV. COMPLEXITY ANALYSIS

In this subsection, the complexity of the proposed SFIC and SIIC detectors is given in term of real flops [28], [29], where one real-valued flop means a real-valued multiplication or addition. The complexity of the proposed SFIC and SIIC detectors is given in (35) and (36) as shown at the bottom of the previous page, respectively, where $b_3 = b_2/N_a$ deontes the number of bits for one GSTSK sybmol.

The details of the complexity of the SFIC detector are given as follows. Specifically, the complexity of the proposed SFIC detector is mainly invoked by (12)-(15). In (12), $\mathbf{B}_l = diag\left(\alpha_1, \alpha_2, \cdots, \alpha_{N_t}\right) \in \mathbb{C}^{N_t \times N_t}$ is a diag matrix, which has only N_t non-zero real elements. $\hat{\mathbf{X}}_l \in \mathbb{C}^{N_t \times T}$ is a matrix, which has $N_t T$ non-zero complex elements. Here, the operation of a real element multiplying by a complex element needs 2 flops, while the operation of complex subtraction needs 2 flops. Thus $\mathbf{B}_l\hat{\mathbf{X}}_l$ needs $2N_tT$ flops and $\tilde{\mathbf{X}}_l - \mathbf{B}_l\hat{\mathbf{X}}_l$ needs $2N_tT$ flops. The above two operations $\mathbf{B}_l\hat{\mathbf{X}}_l$ and $\tilde{\mathbf{X}}_l - \mathbf{B}_l\hat{\mathbf{X}}_l$ need to compute N times since the index l of subcarrier is traversed from 1 to N. So the number of flops for calculating $\hat{\mathbf{D}}_l$ is $4N_tT$ flops. The number of flops for other equations (13)-(15) is computed in the similar way.

V. SIMULATION RESULTS

In this section, the proposed detectors are simulated to show their performance in GSTFIM systems. First, the convergence of the proposed detectors are analysed by the extrinsic information transfer (EXIT) performance chart [30]. Then the bit error rate (BER) of the proposed SFIC and SIIC detectors has been given. In order to get the baseline, the maximum likelihood (ML) detector without clipping (''IDEAL'') and ML detector with clipping (''WORST'') have been simulated in the follows. Moreover, Extended Vehicular A (EVA) channel model [31] and QPSK modulation are employed for the GSTFIM systems. 1/2 rate RSC recursive convolution code is employed for channel coding, and the octonary generating binomial is $[7 \quad 5]_8$.

Figs. 3 and 4 give the EXIT performance charts of the proposed detectors in the symmetric channel ($N_t = 2, N_r = 2$) and asymmetric channel ($N_t = 2, N_r = 4$), respectively, where I_A denotes the correlation between the input bit information and the original transmitted bit information, I_E denotes the correlation between the output bit information and the original transmitted bit information. The parameters of Fig. 3 are as follows: $N = 128, K = 64, N_b = 2, N_a = 1, Q = 4, L = 2, \gamma = -2dB$, while the parameters of Fig. 4 are: $N = 64, K = 32, N_b = 2, N_a = 1, Q = 4, L = 2, \gamma = -3dB$. As can be observed in Figs. 3 and 4, the SIIC detector can provide more extrinsic information compared to SFIC, thus it can achieve better

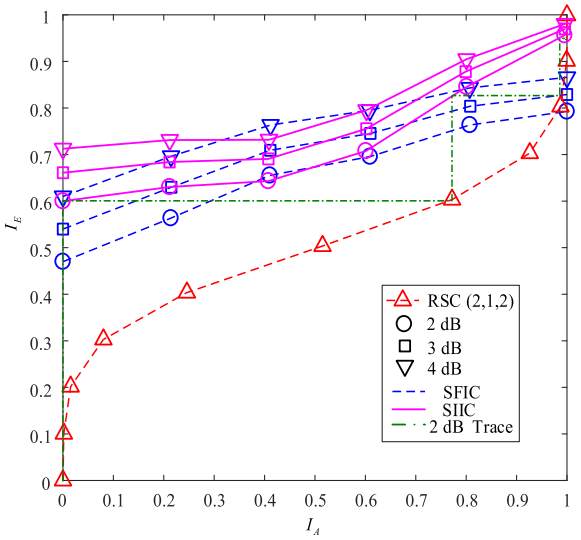

FIGURE 3. EXIT chart of the proposed SFIC and SIIC detectors for GSTFIM systems with $N_t = 2$, $N_r = 2$.

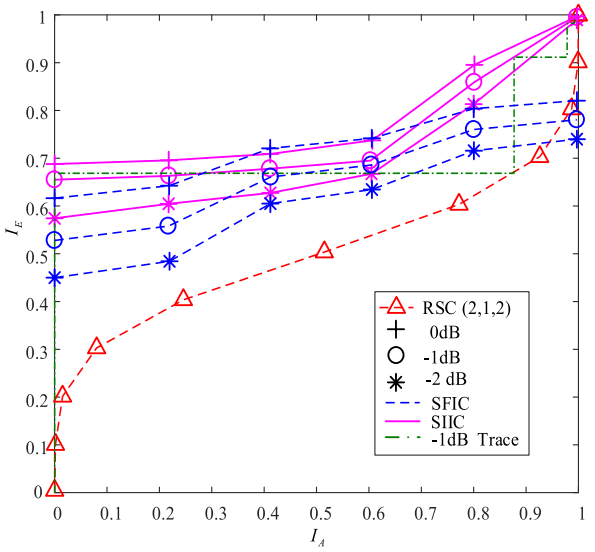

FIGURE 4. EXIT chart of the proposed SFIC and SIIC detectors for GSTFIM systems with $N_t = 2$, $N_r = 4$.

BER performance. Furthermore, the trace line based on extrinsic information transfer and EXIT curve of RSC are given in Figs 3 and 4. As can be described, in the SIIC detector, after a maximum of four vertical coordinate jumps, the correlation degree between the output bit information and the original transmitted bit information is approximately equal to 1, that is, the detector can converge within four iterations.

Then Figs. 5 and 6 compare the BER performance of the proposed SFIC and SIIC detectors for GSTFIM systems, whose system parameters are identical to Figs. 3 and 4, respectively. It is consistent with the external information transfer curve presented in Figs 5 and 6, and we confirm that the SIIC detector has better BER performance than SFIC due to the fact that it has employed the mean and variance of the GSTFIM symbol to estimate the mean and variance of

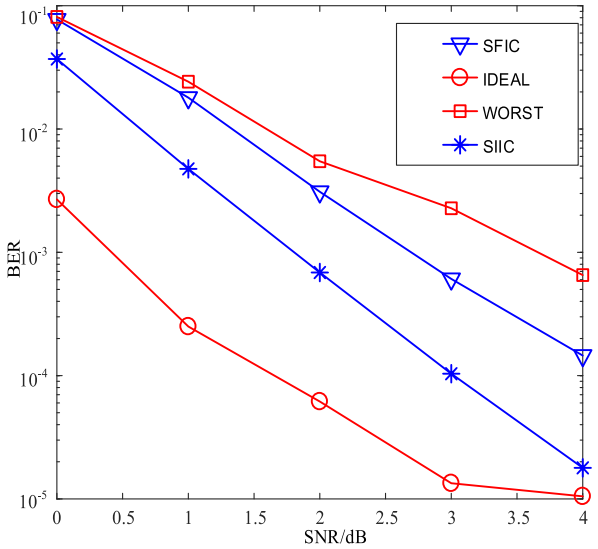

FIGURE 5. BER comparisons of the proposed SFIC and SIIC detectors for GSTFIM systems with $N_t = 2,\ N_r = 2$.

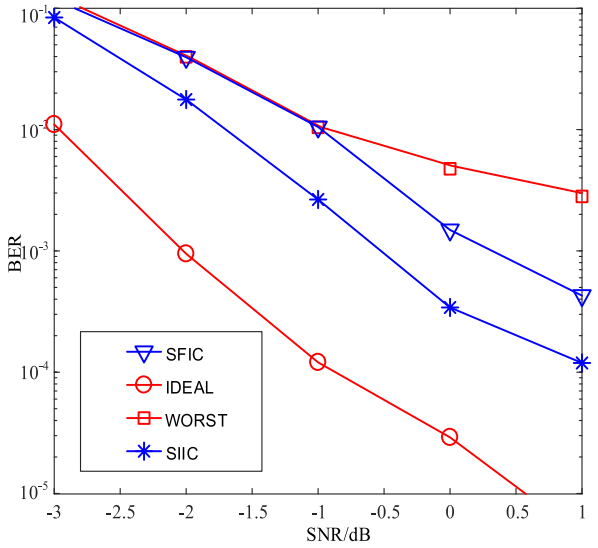

FIGURE 6. BER comparisons of the proposed SFIC and SIIC detectors for GSTFIM systems with $N_t = 2,\ N_r = 4$.

clipping noise components, and can reconstruct the interference more accurately. Specifically, the SFIC detector has a performance gain of about 1 dB compared with the WORST detector at BER= 10^{-3}, and the SIIC detector has a performance gap of about 1 dB compared with the IDEAL detector at BER= 10^{-3}.

Based on the complexity analysis in Section IV, the single iteration complexity of the proposed detectors, whose system parameters are identical to Figs. 3 and 4, is given in Fig. 7. Specifically, the SFIC detector is capable of achieving a 48% complexity reduction as opposed to SIIC with $N_t = 2,\ N_r = 2$, while is capable of achieving a 32% complexity reduction with $N_t = 2,\ N_r = 4$.

In general, the SIIC detector can achieve better interference cancellation performance than SFIC, but consumes higher complexity. Thus, according to the specific

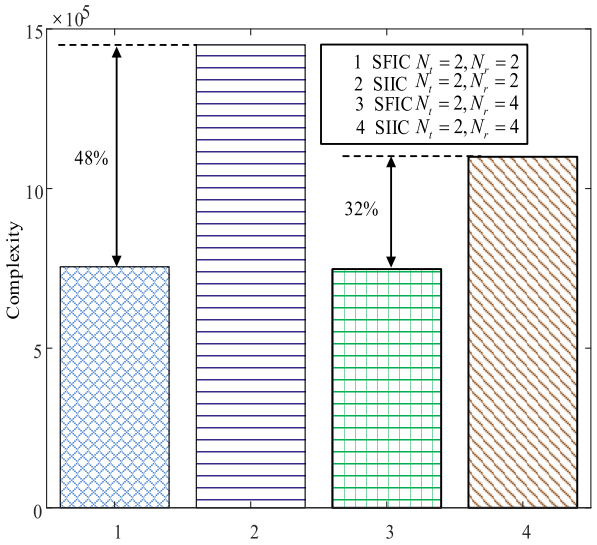

FIGURE 7. Complexity comparisons of the proposed SFIC and SIIC detectors for GSTFIM systems.

communication scenarios, we can flexibly select the appropriate detector for canceling the clipping interference.

VI. CONCLUSION

In this paper, for alleviating the influence of clipping operation toward generalized space-time-frequency index modulation systems, a pair of new detectors were proposed. The proposed SIIC detector can achieve better performance compared to the proposed SFIC detector. Moreover, the proposed detectors are capable of meeting different communication scenarios and offering a flexible tradeoff between system performance and computational complexity.

REFERENCES

[1] Y. Li, J. H. Winters, and N. R. Sollenberger, "MIMO-OFDM for wireless communications, signal detection with enhanced channel estimation," *IEEE Trans. Commun.*, vol. 50, no. 9, pp. 1471–1477, Sep. 2002.
[2] P. Xia, S. Zhou, and G. Giannakis, "Adaptive MIMO-OFDM based on partial channel state information," *IEEE Trans. Signal Process.*, vol. 52, no. 1, pp. 202–213, Jan. 2004.
[3] A. Pascual-Iserte, A. Perez-Neira, and M. Lagunas, "On power allocation strategies for maximum signal to noise and interference ratio in an OFDM-MIMO system," *IEEE Trans. Wireless Commun.*, vol. 3, no. 3, pp. 808–820, May 2004.
[4] X. Cheng, K. Xu, and S. Li, "Compensation of phase noise in uplink massive MIMO OFDM systems," *IEEE Trans. Wireless Commun.*, vol. 18, no. 3, pp. 1764–1778, Mar. 2019.
[5] M. I. Kadir, "Generalized space-time-frequency index modulation," *IEEE Commun. Lett.*, vol. 23, no. 2, pp. 250–253, Feb. 2019.
[6] R. Y. Mesleh, H. Haas, and S. Sinanovic, "Spatial modulation," *IEEE Trans. Veh. Technol.*, vol. 57, no. 4, pp. 2228–2241, Jul. 2008.
[7] M. Di Renzo, H. Haas, A. Ghrayeb, S. Sugiura, and L. Hanzo, "Spatial modulation for generalized MIMO: Challenges, opportunities, and implementation," *Proc. IEEE*, vol. 102, no. 1, pp. 56–103, Jan. 2014.
[8] P. Yang, M. Di Renzo, and Y. Xiao, "Design guidelines for spatial modulation," *IEEE Commun. Surveys Tuts.*, vol. 17, no. 1, pp. 6–26, May 2014.
[9] E. Basar, U. Aygolu, E. Panayirci, and H. V. Poor, "Orthogonal frequency division multiplexing with index modulation," *IEEE Trans. Signal Process.*, vol. 61, no. 22, pp. 5536–5549, Nov. 2012.
[10] Y. Xiao, S. Wang, L. Dan, X. Lei, P. Yang, and W. Xiang, "OFDM with interleaved subcarrier-index modulation," *IEEE Commun. Lett.*, vol. 18, no. 8, pp. 1447–1450, Aug. 2014.
[11] E. Basar, M. Wen, R. Mesleh, M. Di Renzo, Y. Xiao, and H. Haas, "Index modulation techniques for next-generation wireless networks," *IEEE Access*, vol. 5, pp. 16693–16746, 2017.

[12] P. Yang, Y. Xiao, Y. L. Guan, M. Di Renzo, S. Li, and L. Hanzo, "Multidomain index modulation for vehicular and railway communications: A survey of novel techniques," *IEEE Veh. Technol. Mag.*, vol. 13, no. 3, pp. 124–134, Sep. 2018.
[13] P. Yang, Y. Xiao, M. Xiao, and S. Li, "6G wireless communications: Vision and potential techniques," *IEEE Netw.*, vol. 33, no. 4, pp. 70–75, Jul. 2019.
[14] R. Yoshizawa and H. Ochiai, "Trellis-assisted constellation subset selection for PAPR reduction of OFDM signals," *IEEE Trans. Veh. Technol.*, vol. 66, no. 3, pp. 2183–2198, Mar. 2017.
[15] Y. Wang, W. Chen, and C. Tellambura, "A PAPR reduction method based on artificial bee colony algorithm for OFDM signals," *IEEE Trans. Wireless Commun.*, vol. 9, no. 10, pp. 2994–2999, Oct. 2010.
[16] C.-P. Li, S.-H. Wang, and C.-L. Wang, "Novel low-complexity SLM schemes for PAPR reduction in OFDM systems," *IEEE Trans. Signal Process.*, vol. 58, no. 5, pp. 2916–2921, May 2010.
[17] X. Li and L. J. Cimini, "Effects of clipping and filtering on the performance of OFDM," in *Proc. IEEE 47th Veh. Technol. Conf.*, vol. 3, May 1997, pp. 1634–1638.
[18] J. Armstrong, "Peak-to-average power reduction for OFDM by repeated clipping and frequency domain filtering," *Electron. Lett.*, vol. 38, no. 5, pp. 246–247, May 2002.
[19] H. Ochiai and H. Imai, "Performance analysis of deliberately clipped OFDM signals," *IEEE Trans. Commun.*, vol. 50, no. 1, pp. 89–101, Jan. 2002.
[20] Y. Xiao, S. Li, X. Lei, and Y. Tang, "Clipping noise mitigation for channel estimation in OFDM systems," *IEEE Commun. Lett.*, vol. 10, no. 6, pp. 474–476, Jun. 2006.
[21] L. Yang, X. Lin, X. Ma, and S. Li, "Iterative clipping noise elimination of clipped and filtered SCMA-OFDM system," *IEEE Access*, vol. 6, pp. 54427–54434, 2018.
[22] S. Liang, J. Tong, and L. Ping, "On iterative compensation of clipping distortion in OFDM systems," *IEEE Wireless Commun. Lett.*, vol. 8, no. 2, pp. 436–439, Apr. 2019.
[23] K. Anoh, C. Tanriover, and B. Adebisi, "On the optimization of iterative clipping and filtering for PAPR reduction in OFDM systems," *IEEE Access*, vol. 5, pp. 12004–12013, 2017.
[24] F. Yang, J. Gao, S. Liu, and J. Song, "Clipping noise elimination for OFDM systems by compressed sensing with partially aware support," *IEEE Trans. Broadcast.*, vol. 63, no. 1, pp. 103–110, Mar. 2017.
[25] L. Yang, K. Song, and Y. M. Siu, "Iterative clipping noise recovery of OFDM signals based on compressed sensing," *IEEE Trans. Broadcast.*, vol. 63, no. 4, pp. 706–713, Dec. 2017.
[26] Y. Zhao, Y. Xiao, P. Yang, S. Fang, and W. Xiang, "Iterative compensation for clipping noise in spatial modulation OFDM systems," *IEEE Trans. Veh. Technol.*, vol. 68, no. 12, pp. 12422–12426, Dec. 2019, doi: 10.1109/tvt.2019.2947193.
[27] S. Sugiura, S. Chen, and L. Hanzo, "Generalized space-time shift keying designed for flexible diversity-, multiplexing- and complexity-tradeoffs," *IEEE Trans. Wireless Commun.*, vol. 10, no. 4, pp. 1144–1153, Apr. 2011.
[28] L. Xiao, P. Yang, Y. Xiao, S. Fan, M. Di Renzo, W. Xiang, and S. Li, "Efficient compressive sensing detectors for generalized spatial modulation systems," *IEEE Trans. Veh. Technol.*, vol. 66, no. 2, pp. 1284–1298, Feb. 2017.
[29] S. Fan, Y. Xiao, L. Xiao, P. Yang, R. Shi, and K. Deng, "Improved layered message passing algorithms for large-scale generalized spatial modulation systems," *IEEE Wireless Commun. Lett.*, vol. 7, no. 1, pp. 66–69, Feb. 2018.
[30] M. El-Hajjar and L. Hanzo, "EXIT charts for system design and analysis," *IEEE Commun. Surveys Tuts.*, vol. 16, no. 1, pp. 127–153, May 2014.
[31] *E-UTRA Base Station (BS) Radio Transmission and Reception (Released8)*, document TSG-RAN 36.104, Rev. 8.5.0, 3GPP, 2009.
[32] J. Wang and S. Li, "Soft versus hard interference cancellation in MMSE OSIC MIMO detector: A comparative study," in *Proc. 4th Int. Symp. Wireless Commun. Syst.*, Oct. 2007, pp. 642–646.
[33] N. Du and D. Xu, "Low complexity iterative receiver for MIMO-OFDM systems," in *Proc. Int. Symp. Int. Signal Process. Commun. Syst. (SPACS)*, Nov. 2007, pp. 622–625.
[34] J. Zeng, J. Lin, and Z. Wang, "Low complexity message passing detection algorithm for large-scale MIMO systems," *IEEE Wireless Commun. Lett.*, vol. 7, no. 5, pp. 708–711, Oct. 2018.
[35] S. Wu, L. Kuang, Z. Ni, J. Lu, D. Huang, and Q. Guo, "Low-complexity iterative detection for large-scale multiuser MIMO-OFDM systems using approximate message passing," *IEEE J. Sel. Topics Signal Process.*, vol. 8, no. 5, pp. 902–915, Oct. 2014.

SHIWEN FAN received the B.S. degree from the University of Electronic Science and Technology of China (UESTC), Chengdu, China, in 2013, where he is currently pursuing the Ph.D. degree with the National Key Laboratory of Science and Technology on Communications. His research is in the field of wireless communications and communication theory. In particular, he is very interested in signal detection of wireless communication systems.

YUE XIAO received the Ph.D. degree in communication and information systems from the University of Electronic Science and Technology of China (UESTC), in 2007. He is currently a Professor with the National Key Laboratory of Science and Technology on Communications, UESTC. He has published more than 100 international journals and has been in charge of more than 20 projects in the area of Chinese 3G/4G/5G wireless communication systems. He is also an Inventor of more than 50 Chinese and PCT patents on wireless systems. His research interests are in system design and signal processing toward future wireless communication systems. He serves as an Associate Editor for the IEEE COMMUNICATIONS LETTERS.

SHU FANG received the B.S. degree from the University of Electronic Science and Technology of China, in 2003, and the Ph.D. degree from the Beijing University of Posts and Telecommunications, China, in 2008. From July 2011 to March 2012, she was a Research Fellow with the School of Electrical and Electronic Engineering, Nanyang Technological University, Singapore. She is currently an Associate Professor with the Department of National Key Laboratory on Communications, University of Electronic Science and Technology of China. Her research interests are in the areas of wireless communications, signal processing, digital communications, and next-generation networks.

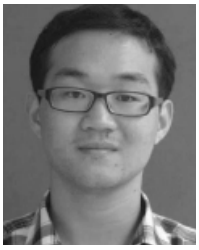

YAN ZHAO received the B.E. degree in communication engineering from Zhengzhou University, Zhengzhou, China, in 2012, and the Ph.D. degree in communication and information systems from the University of Electronic Science and Technology of China (UESTC), in 2019. From 2017 to 2018, he was a Visiting Student with the School of Electronics and Computer Science, University of Southampton, Southampton, U.K. His research interests include MIMO systems, nonorthogonal multiple access, and communication signal processing.

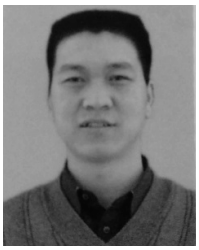

XIAOTIAN ZHOU is currently a Researcher with the Science and Technology on Communication Networks Laboratory, The 54th Research Institute of China Electronics Technology Group Corporation (CETC). His research is in the field of 5G wireless communications. In particular, he is very interested in signal processing of massive multiple input and multiple output (MIMO) systems.